



## A comparative compositional study of Egyptian glass from Amarna with regard to cobalt sources and other colourants

Anna K. Hodgkinson<sup>a,b,\*</sup>, Quentin Lemasson<sup>c,d</sup>, Michael Mäder<sup>e</sup>, Frans Munnik<sup>f</sup>, Laurent Pichon<sup>c,d</sup>, Stefan Röhrs<sup>g</sup>, Ina Reiche<sup>d,g,h</sup>

<sup>a</sup> Excellence Cluster TOPOI, Berlin, Germany

<sup>b</sup> Ägyptologisches Seminar, Freie Universität Berlin, Fabeckstr. 23-25, 14195 Berlin, Germany

<sup>c</sup> Centre de recherche et de restauration des musées de France (C2RMF), 14 quai François Mitterrand, 75001 Paris, France

<sup>d</sup> Lab-BC UAR 3506 CNRS-C2RMF-Chimie Paristech/PSL University, C2RMF, 14 quai François Mitterrand, 75001 Paris, France

<sup>e</sup> Dresden State Art Collections, Taschenberg 2, 01067 Dresden, Germany

<sup>f</sup> Helmholtz-Zentrum Dresden-Rossendorf, Ion Beam Center, Bautzner Landstraße 400, 01328 Dresden, Germany

<sup>g</sup> Rathgen-Forschungslabor, Staatliche Museen zu Berlin, Stiftung Preußischer Kulturbesitz, Schloßstraße 1a, 14059 Berlin, Germany

<sup>h</sup> Institut de recherche de Chimie Paris, PCMTH team, UMR 8247 CNRS-Chimie Paristech/PSL University, 11 rue Pierre et Marie Curie, 75005 Paris, France

### ARTICLE INFO

#### Keywords:

Glass  
Amarna  
Egypt  
PIXE  
PIGE  
RBS  
microPIXE-imaging  
Trace elements  
Cobalt sources  
Colourants

### ABSTRACT

A selection of Late Bronze Age glass objects from the site of Amarna (Egypt) was analysed for their overall chemical composition, colourants and transition metals associated with the sources of cobalt ore. The objects were analysed by means of Particle Induced X-Ray and Gamma-ray Emission and Rutherford Backscattering Spectrometry at the IBC, HZDR, Dresden and the New AGLAE facility, C2RMF, Paris. The data was subsequently compared with further measurements obtained by portable X-Ray Fluorescence (and by Laser-Ablation Inductively-Coupled-Plasma Mass-Spectrometry) in order to sound the potential of these non-destructive methods to obtain new insights into the production process of glass from Amarna and its provenancing.

### 1. Introduction and background

A selection of Late Bronze Age glass objects from the site of Amarna in Middle Egypt from the collection of the Egyptian Museum, Berlin (ÄMP) (Fig. 1) was studied by means of PIXE (Particle Induced X-Ray Emission) / PIGE (Particle Induced Gamma-ray Emission) and RBS (Rutherford Backscattering Spectrometry). Since dark blue was a highly popular colour during pharaonic times in Egypt, cobalt coloured glass objects, both finished items and those used for the production of the former, were frequently found in the workshops and houses of the New Kingdom (c. 1550–1069 BCE). The first regular use of glass can be witnessed in Egypt at the beginning of the 18th Dynasty (c. 1550–1290 BCE; Shortland 2012, 49–53; Nicholson, 2007, 3–7). While the manufacture of ornate glass vessels required a higher set of skill, it was possible to produce glass beads at household-level without any complex firing structures (Hodgkinson and Bertram, 2020). The main purpose of

this study was to sound the informative potential of the analytical methods in order to obtain further insights into glass processing and provenancing. In particular, the study aimed to determine whether it is possible to chemically detect the source of the cobalt (Co) ore used for the colouring of the material by PIXE/PIGE. The source of the processed Co-ore that was used in a glass batch is more or less discernible through the correlation of the transition metals nickel (Ni), zinc (Zn) and manganese (Mn), some light elements, including aluminium (Al) and magnesium (Mg) (Abe et al., 2012; Shortland et al., 2006) as well as some Rare Earth Elements (REEs: see Hodgkinson and Frick, 2020a and 2020b; cf. Lankton et al., 2022). The main source of Co used during the 18th Dynasty was the area of the oases Kharga and Dakhla in the Egyptian Western Desert (Kaczmarczyk, 1986). It has been recognised that no uniform chemical pattern exists for this source, but that a variety of subgroups are discernible, according to various geological sources in the same area (Smirniou and Rehren, 2013). Simultaneously, all glass

\* Corresponding author.

E-mail address: [a.hodgkinson@fu-berlin.de](mailto:a.hodgkinson@fu-berlin.de) (A.K. Hodgkinson).

<https://doi.org/10.1016/j.jasrep.2024.104412>

Received 18 September 2023; Received in revised form 11 January 2024; Accepted 24 January 2024

Available online 17 February 2024

2352-409X/© 2024 The Authors. Published by Elsevier Ltd. This is an open access article under the CC BY license (<http://creativecommons.org/licenses/by/4.0/>).

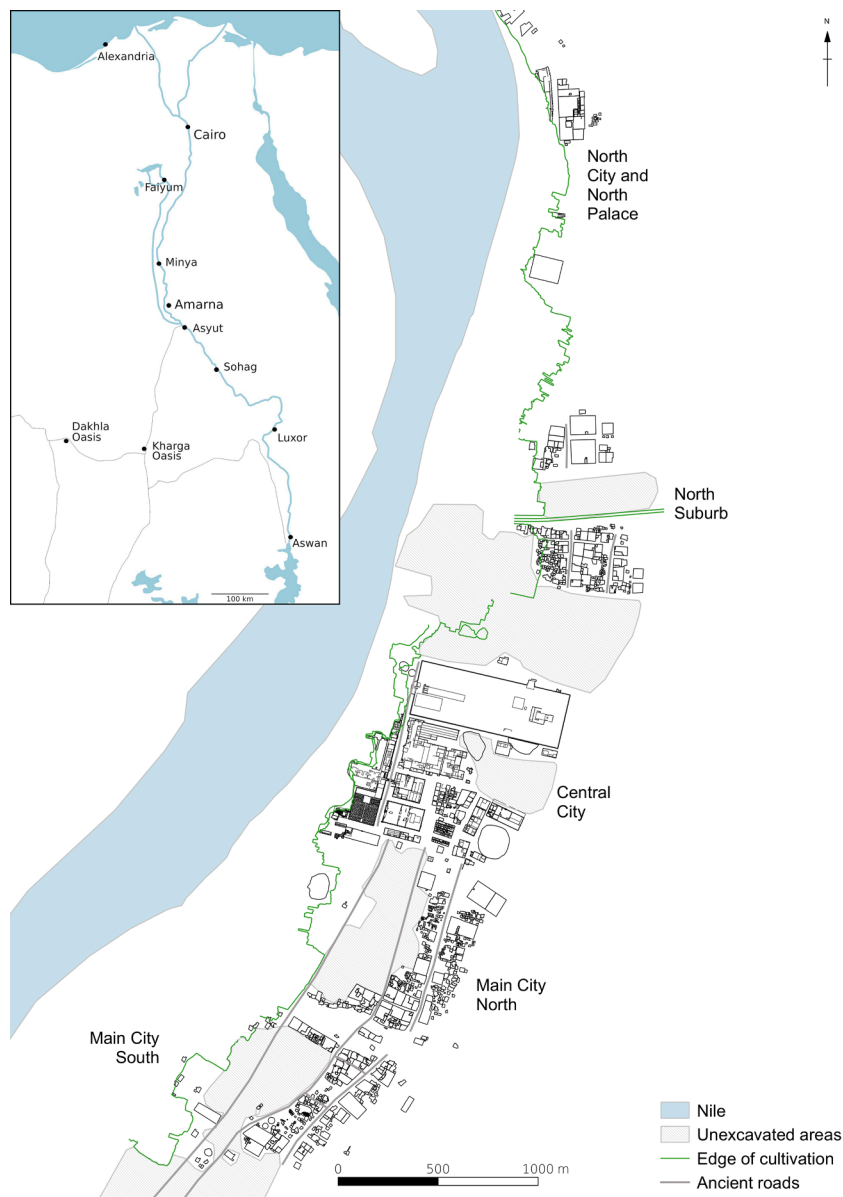


Fig. 1. Map of Amarna with an inset of the location of Amarna in Egypt. Map: A. K. Hodgkinson/FU Berlin, based on data from Kemp and Garfi, 1993.

objects coloured with Co-ore from this region have low potassium values together with high aluminium and magnesium (Nicholson, 2007, 97).

A team led by Y. Abe achieved a classification of the various geological cobalt sources found in Egyptian vitreous products by means of transition metals (Ni, Zn, Mn) analysis by portable X-Ray Fluorescence (pXRF: Abe et al., 2012). The samples analysed by Abe and colleagues include glass and faience objects recently excavated at Dahshur North and North-west Saqqara and kept in Egypt in addition to some objects in two museum collections in Japan dating to the 18th and the 19th/20th dynasties. This means that the objects overlap with those from Amarna and the subsequent periods in terms of chronology. In order to gain information on light elements in the glass, PIXE/PIGE and RBS analyses were conducted at the Ion Beam Center (IBC) Helmholtz-Zentrum Dresden-Rossendorf (HZDR) and at the New AGLAE microfocuss beamline at the AGLAE accelerator, C2RMF in Paris, respectively, on a selection of glass objects from the collection of the ÄMP. While the objects in the museum collection are not provenanced more precisely than to the site of Amarna in general, they were available for these analyses in Europe, it being illegal to export the well-provenanced material from Egypt and PIXE/PIGE technology not currently being available in Egypt.

Approximately 500 more precisely provenanced blue glass objects from recently excavated workshop sites were analysed in the excavation house at Amarna using a pXRF device (ELIO by XGLab). Through this, it was possible to create object groups based on provenance, using semi-quantitative elemental analysis. It has also been possible to identify the western desert as the source of the Co-ore through the (partially elevated) presence of Zn, Ni, Mn and Fe (Hodgkinson et al., 2019a and 2019b). However, the instrument used by Hodgkinson was unable to detect neither the light elements (in particular Al, Mg) nor the REEs, which would have provided further information regarding possible variations in the cobalt source.

Forty glass objects from the collection of the ÄMP and two Co-ore samples from the region of Ain Asil (near Dakhla Oasis) had previously been analysed by Laser-Ablation Inductively-Coupled-Plasma Mass-Spectrometry (LA-ICP-MS) at the Geoforschungszentrum in Potsdam (GFZ), the same objects having previously been analysed using the ELIO pXRF device. These analyses achieved a validation of the pXRF data obtained for the transition metals (Co, Ni, Zn and Mn) between both sets of analysis, and thus also confirmed the reliability of the transition metal data previously obtained at Amarna (see Hodgkinson et al., 2019a



glass mixture or added to an un-coloured base glass (see Shortland et al., 2006; Rehren, 2001). Simultaneously, the ceramic sherd with the blue glassy matrix and the quartz fragments (ÄM 21977, see Fig. 2) may or may not have been used in the manufacture of glass (see Shortland, 2012, 120 for a summary of the reconstructed glass-making process). With regard to glass-working, finished glass ingots would have been broken up into chips from which rods and bars were drawn. While glass rods were used both for the manufacture of beads and for the decoration of polychrome glass vessels, flat glass bars were often carved using cold-working techniques, and turned into inlays. Please refer to the supplementary material for an overview of how the objects analysed for this paper fit into the New Kingdom Egyptian *chaîne opératoire* of glass making and -working. While numerous glass objects were coloured by Co, a large number of Co-Cu coloured objects also exist, and they have been grouped according to the definition set by Smirniou and Rehren (2013; see table S1). Since the same transition metal correlations are known to exist for these, Co-Cu coloured objects have been defined as containing both metals, but not been extracted from this study (Smirniou and Rehren, 2013; Hodgkinson et al., 2019a).

## 2.2. Methods 1: The set-up at IBC, HZDR

External PIXE, PIGE and RBS were performed simultaneously using a 4 MeV proton beam. The ion beam is extracted from vacuum through a 2 µm Havar (Co-alloy) foil and passes through a largely enclosed space with a continuous helium (He) flow to reach the samples with an energy of about 3.85 MeV. The analysed area is 1 mm in diameter and the ion beam current is less than 0.5 nA. For PIXE, two Si(Li) detectors were used, one with an active area of 12 mm<sup>2</sup>, optimised for the detection of light elements (Al – Fe) for which the path to the detector is also enclosed within a helium flow to minimise X-ray losses. The other detector is optimised for heavier elements (Fe – U) for which it has a large active area of 80 mm<sup>2</sup> and a thickness of 5 mm to maximise the detection of high energy X-rays with low cross-sections. For PIGE, a high purity Ge detector with a relative efficiency of 60 % at 1.3 MeV was used to detect the gamma-rays from light elements including Li, B, F, Na, Mg, Al, and Si. For RBS, a 100 mm<sup>2</sup> PIPS detector was used to detect the back-scattered ions at a scattering angle of 135° with respect to the ion beam. RBS with 4 MeV protons is also sensitive for C, N and O because the non-Rutherford cross-sections in this energy range are much larger than the Rutherford cross-sections.

The analysis of the PIXE spectra was performed with GupixWin v2.2.3 (Campbell et al., 2000; Campbell et al., 2010) assuming a thick homogeneous sample with all elements present as oxides. Thick Al, MgO and Ag samples and a sample with a thin Ni layer were used to check the detector efficiency and calculate the H factor (solid angle) for both PIXE detectors. Four reference glasses, the Corning/Brill A and B, and NBS 610 and 612 were used as validation of the calibration. For the Corning glasses, recommended values were used that are presented in Wagner et al., 2012, which originate from Brill, 1999 and Vicenzi et al., 2002, supplemented with some new values. It should be noted that these are not certified values. The Al, MgO and Corning A standards were also used as the calibration samples for the PIGE calculation of the Al, Mg and Al concentrations, respectively, according to the procedure described in Chapter 7 of (Wang and Nastasi, 2009). The final concentrations are the combination of the results for Na, Mg and Al from PIGE, Si – Mn from the low energy PIXE detector, Fe – Pb from the high-E PIXE detector and O calculated from the other elements according to the stoichiometry. The RBS spectra were analysed using the program NDF (Barradas et al., 1997). All analyses require the stopping powers of ions in matter for which the SRIM-2013 stopping powers are used (Ziegler et al., 2010). The RBS spectra were analysed separately to check for corrosion. Measured cross-sections were used for the analysis for most elements because the cross-sections for light elements are non-Rutherford for a high energy proton beam.

## 2.3. Methods 2: The New AGLAE set-up

External micro-PIXE/PIGE was performed simultaneously with 3 MeV protons with an intensity of 3 to 4 nA under a He atmosphere directly on the objects without invasive sampling at the New AGLAE accelerator microfocus beamline at the AGLAE accelerator, installed in the C2RMF in the Louvre (Paris, France) in 2018 (Pichon et al., 2014). The analysed area measures either 500x500 µm<sup>2</sup> or 1000x1000 µm<sup>2</sup> for averaging the composition. For chemical imaging larger map sizes were measured. PIXE analysis was performed using four SDD detectors: the first one was dedicated to the analysis of low Z elements ( $10 < Z < 29$ ) and a He flux was used to reduce the absorption of incident and remitted beams by air; the three other SDD detectors were dedicated to high Z elements ( $Z > 26$ ) and an Al filter (50 µm) was placed in front of the detector in order to absorb the low energy X-rays. One HPGe detector is used for the PIGE measurement. (Pichon et al., 2014).

For each glass sample at least two measurements were performed. In addition, PIXE/PIGE on a larger area was performed on the layered glass sample (ÄM 40418; see table S1) in order to obtain distribution images of the different elements contained in the different glass layers. The beam current was limited in order to lower the 1 nC and to ensure safe analysis conditions of the glass objects without visible modification under the beam.

The PIXE spectra were extracted using GUPIX software combined with TRAUPIXE software developed at New AGLAE (Pichon et al., 2015), assuming that analysed zones are homogeneous and that all elements are present as oxides. The geochemical diorite DR-N sample and the Brill/Corning A, B and D glass standards were used as reference materials in order to calibrate the PIGE data and control PIXE results (Vicenzi et al., 2002). The compositions given in this paper result from the combination of PIXE data and the sodium (Na) content obtained by PIGE using its characteristic gamma line at 440 keV.

## 3. Results: The chemical composition of the Amarna glass objects

### 3.1. Homogeneity of the glass composition at the surface?

The RBS analysis carried out at HZDR can be used to verify the homogeneity of the glass composition at the surface and to highlight potential differences between the corroded surface and the core glass of an object. Some examples of spectra are shown in Fig. 3A. The compositional changes caused by corrosion are related to the surface of the glass and this is found at the higher energies in the RBS spectrum as indicated by the arrows in Fig. 3A. Sample ÄM 39040 shows a normal glass spectrum, whereas samples ÄM 40043 and ÄM 36902 show weathering / corrosion of the surface. The effects of corrosion result in a decrease in alkali metals such as Na and K. In correspondence, the concentration of SiO<sub>2</sub> will increase and, therefore, the overall O concentration at the surface will increase (Mäder and Neelmeijer, 2004). The reduction of Na and increase of O is clearly visible, although a reduction of K has not been observed. Sample ÄM 40057 shows a normal glass spectrum but with an increase of C at the surface.

An example of a detailed analysis of a RBS spectrum for the corrosion spot on sample ÄM 36902 is shown in Fig. 3B. A simulation of the spectrum was calculated based on a sample model with three layers: the first layer contains only C and O, the second layer contains no Na and has increased concentrations of O and Si, while the third layer represents uncorroded glass. The coloured curves in Fig. 3B represent the contributions of each element to the simulation, e.g. the green curve represents C near the surface. Na is not present in a corroded surface layer, which is in the region of channels 340 to 370 (extension of the pink curve). The thickness of the corrosion layer is about 5½ µm, assuming a density of 2.5 g/cm<sup>3</sup>, which is necessary for the calculation of the thickness. The variations in the elemental curves (e.g. the wiggles for Si) were mostly caused by changes in the non-

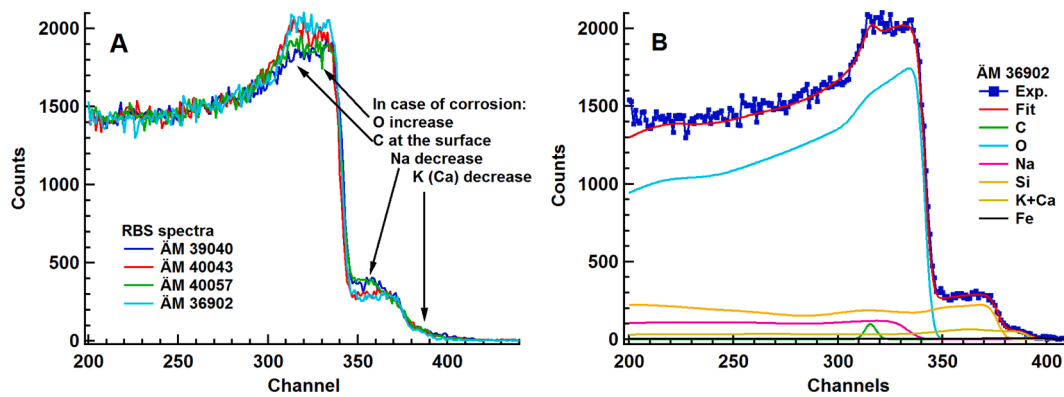


Fig. 3. (A) RBS spectra for four samples, and (B) for sample  $\ddot{A}M$  36,902 (blue points) together with a simulation (red curve). Graphs: F. Munnik/HZDR. (For interpretation of the references to colour in this figure legend, the reader is referred to the web version of this article.)

Rutherford cross-sections but also by changes in the concentration (e.g. for O around channel 310).

Overall, the RBS spectra show various states of corrosion from very little to a corroded surface layer up to 10  $\mu\text{m}$ , especially where Na has leached out. This is an indication for strong variations in local storage conditions. This result is of importance since it indicates that the condition of the surface needs to be taken into consideration when performing non-invasive analysis of archaeological glass objects: since light element concentrations are much more affected by the surface corrosion, transition metals are better suited for provenancing the Co source than light elements.

### 3.2. MicroPIXE-imaging

Micro-PIXE imaging on selected samples was carried out to determine whether the trace element (transition metal) distribution in the glass samples is homogeneous. Indeed, imaging of the blue glass samples carried out at New AGLAE showed a homogeneous elemental distribution pattern at the scale of tens of micron spatial resolution at major, minor and trace element level, i.e. the Co colourant in the blue, etc., but also of the glass matrix on the surface of the object (Na, Mg, Al, Si, K and Ca expressed as oxides, see Fig. 2:  $\ddot{A}M$  39757). Only the Ca map shows some very localised micro-inclusions in an otherwise relatively homogeneous matrix. Therefore, point analysis appears to be sufficient to characterise the type of glass and can be used for inferring information about raw materials used in the production of glass. Further quantitative chemical maps can be found in the [supplementary material](#) (see Figs. S1-S4: objects  $\ddot{A}M$  39757,  $\ddot{A}M$  40060,  $\ddot{A}M$  36899 and  $\ddot{A}M$  36900).

MicroPIXE-imaging is of value for the study of polychrome objects, since it shows the different characteristic minor and trace elements as a function of the observed colours. The example of the striped red, white and blue glass object  $\ddot{A}M$  40418, although probably from a later period, highlights the analytical performances of microPIXE-imaging (see Fig. 4). In the red part Fe, Cu and Pb are found to dominate, an observation consistent with other red glass objects from Amarna. The white strip corresponds to an area rich in Sn and Pb (with a ratio of 1:1, at 6 wt. % each, see table S2). In addition, this strip is not richer in Fe than the other coloured zones. This result is different from what was observed in the white glass sample from Amarna ( $\ddot{A}M$  40346), the latter being white because of the presence of a Ca-Sb-based opacifier. The presence of Sn in the white stripe points towards the use of a Sn-based opacifier as was used in Egypt during the later Roman Period (see [Matin, 2019](#); cf. [Tite et al., 2008](#)). The blue zone corresponds to a Co-based colourant. Similar to the Co-ore used during the Amarna Period, the Co is accompanied by transition metals: while Mn is elevated (as is Fe), both traces of Ni and Zn are present, albeit depleted in the Co used to colour this object (cf. table S2).

### 3.3. Colouring elements identified by means of PIXE technology in glass samples of other colours and polychrome glass

Further glass samples of turquoise, green, yellow, orange, red, violet colour as well as white and colourless glass objects from Amarna were analysed by means of PIXE (table S2). As with the Co blue glass objects from Amarna, these are in correspondence to soda-lime-silica glasses from the 18th Dynasty ([Shortland and Eremin, 2006](#)). The origin of these objects' colour can be determined according to their minor element contents as follows:

Two turquoise glasses analysed at New AGLAE contain between 0.4 and 1 wt. % of CuO which is responsible for the turquoise colour. They are also somewhat rich in  $\text{Sb}_2\text{O}_5$ , with contents ranging between 1.5 and 2.5 wt. %, indicating that they were opacified using antimonate. These objects also contain elevated  $\text{K}_2\text{O}$  (ranging between 1.1 and 2.6 wt. %), which is in line with non-Co-coloured glasses of the Egyptian New Kingdom ([Smirniou and Rehren, 2013](#)).

Two green glass objects analysed at New AGLAE and one at HZDR contain fairly high amounts of CuO in the range of 1.1–2.2 wt. % as well as PbO in the range of 1.8–2.5 wt. % and  $\text{K}_2\text{O}$  (ranging between 0.8 and 2.6 wt. %). In addition, the objects have been opacified using  $\text{Sb}_2\text{O}_5$ , which is in the range of 0.3–0.5 wt. %.

The yellow glass object ( $\ddot{A}M$  39691) is rich in PbO (around 4.0 wt. %) and  $\text{Sb}_2\text{O}_5$  (around 0.7 wt. %), while the orange glass sample ( $\ddot{A}M$  39698) contains high levels of PbO (around 2.7 wt. %) and  $\text{Sb}_2\text{O}_5$  (around 0.4 wt. %), but in lower concentrations than in the yellow glass sample ( $\ddot{A}M$  39691). The  $\text{K}_2\text{O}$  content is also relatively high with a content of 2.0 wt. %. These results, again, are in line with those of other yellow glass objects from Amarna and Malqata (see [Shortland and Eremin, 2006](#)), and both of these objects were analysed at New AGLAE.

Two red glass samples analysed at New AGLAE and one at HZDR contain between 3.8 and 4.4 wt. % of CuO, which is responsible for the red colour, and which has been achieved by introducing reducing conditions in the furnace ([Shortland 2012, 118–119](#)). They are also somewhat rich in  $\text{Sb}_2\text{O}_5$  with a content of c. 0.5 wt. %.

Violet, or amethyst-coloured glasses from Amarna owe their colour to the presence of MnO ([Shortland and Eremin, 2006, 592](#)), which varies between 1.2 and 0.2 wt. % for the objects analysed at New AGLAE. They are also fairly rich in  $\text{Na}_2\text{O}$  with a content of about 10.2 ( $\pm 8.1$ ) wt. %, in MgO with a content of about 3.7 ( $\pm 0.6$ ) wt. % and in  $\text{K}_2\text{O}$  with a content of about 2.0 ( $\pm 0.2$ ) wt. %.

The white glass sample from Amarna analysed at New AGLAE is characterised by the presence of small particles of calcium antimonate  $\text{Ca}_2\text{Sb}_2\text{O}_7$  (Sb c. 1 wt. % and CaO 7.5 wt. %), which had been added to the batch as an opacifying agent ([Shortland and Eremin, 2006](#)).

The largely colourless glass sample is characterised by a high CaO content (around 10.6 wt. %) and in consequence also quite rich in SrO

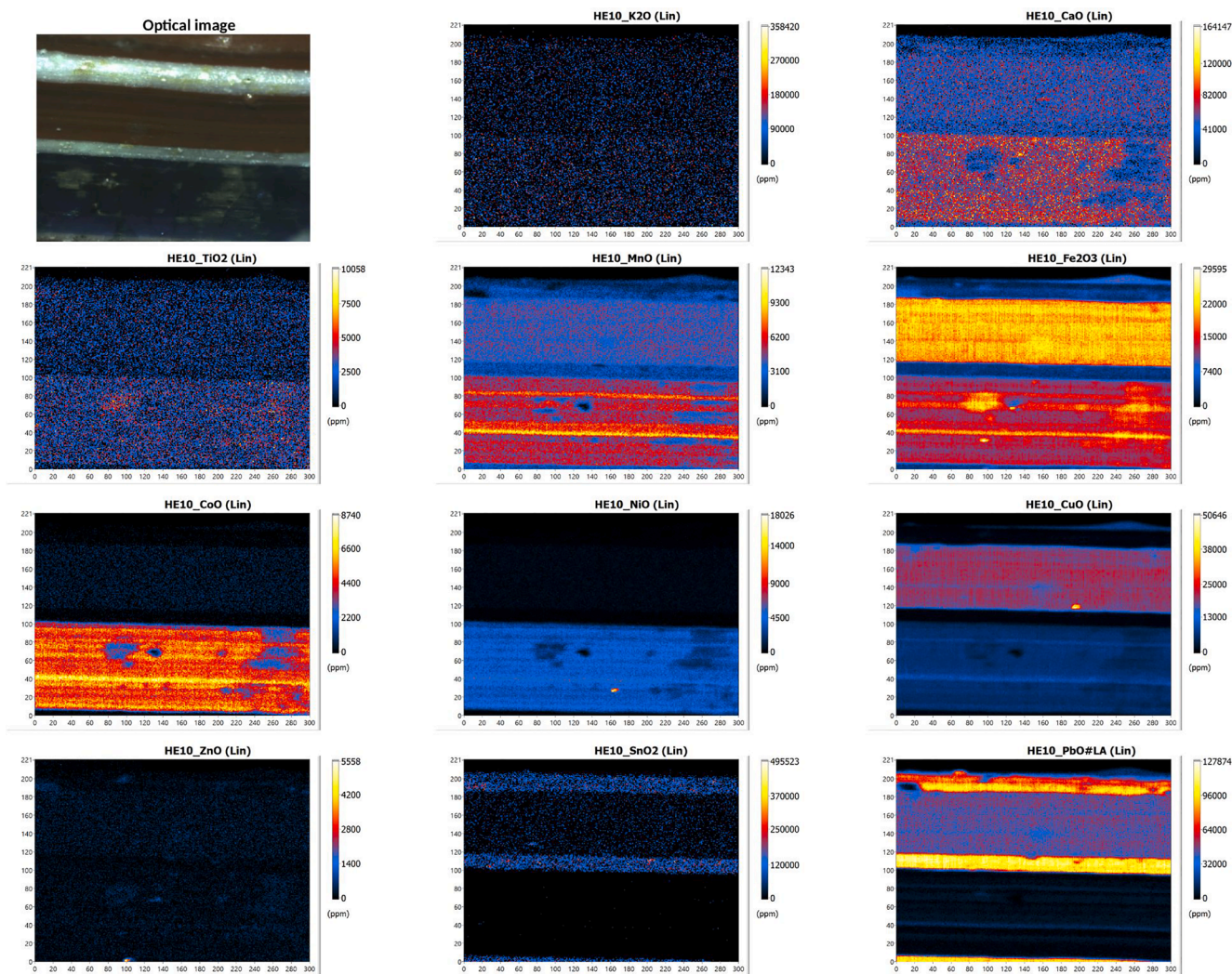


Fig. 4. Qualitative chemical maps of trace elements without the matrix of the striped glass object 40418. Image: L. Pichon/UAR 3506 Lab-BC.

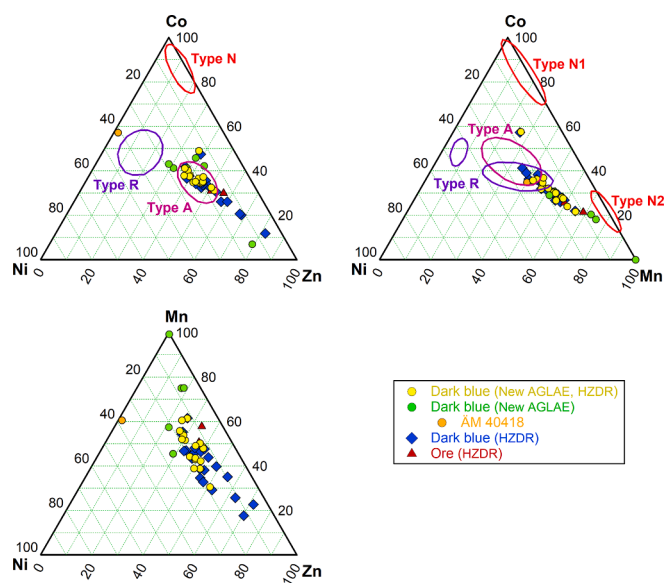


Fig. 5. Ternary diagrams describing the correlation between Co and the transition elements (Ni, Mn, Zn). Graphs: F. Munnik/HZDR.

with a content of about 0.2 wt. %. The blue-green tint of the sample is at least partially due to Fe<sub>2</sub>O<sub>3</sub> impurities (c. 0.6 wt. %).

### 3.4. Analysis of blue glass samples with regard to possible Co sources

The mean composition values for each object determined by microPIXE-PIGE analysis at New AGLAE are presented in table S1 for the blue samples and in table S2 for the glass object of other colours. The blue glass objects from Amarna are typical soda-lime-silica glass of the period. The characteristic blue colour of these glass samples is mainly derived from the processed Co-ore (see Shortland et al., 2006). They contain 64.0 (±3.6) wt. % of SiO<sub>2</sub>, 7.7 (±2.1) wt. % of CaO and 15.7 (±2.7) wt. % of Na<sub>2</sub>O. In terms of minor compounds, they contain on average 2.9 (±0.6) wt. % of MgO, 3.3 (±1.1) wt. % of Al<sub>2</sub>O<sub>3</sub>, 1.2 (±0.7) wt. % of K<sub>2</sub>O and 1.1 (±0.2) wt. % of Cl. With regard to trace elements they contain c. 1.0 wt. % of SO<sub>3</sub>, 0.8 wt. % of Fe<sub>2</sub>O<sub>3</sub>, 0.5 wt. % of Sb<sub>2</sub>O<sub>5</sub>, 0.4 wt. % of P<sub>2</sub>O<sub>5</sub>, 0.3 wt. % of MnO, 0.3 wt. % of CuO, 0.2 wt. % of TiO<sub>2</sub>, 0.2 wt. % of CoO, 0.2 wt. % of ZnO, 0.1 wt. % of SrO and 0.1 wt. % of NiO. These values are in line with those of other Co-coloured glass objects from Egypt from both Malqata and Amarna (Shortland and Eremin, 2006).

The three ternary diagrams shown in Fig. 5 describe the correlation between the Co and the transition metals present in the analysed Co-coloured glass objects. The pattern of the samples in the first two diagrams is similar to that published by Abe and colleagues (Abe et al.,

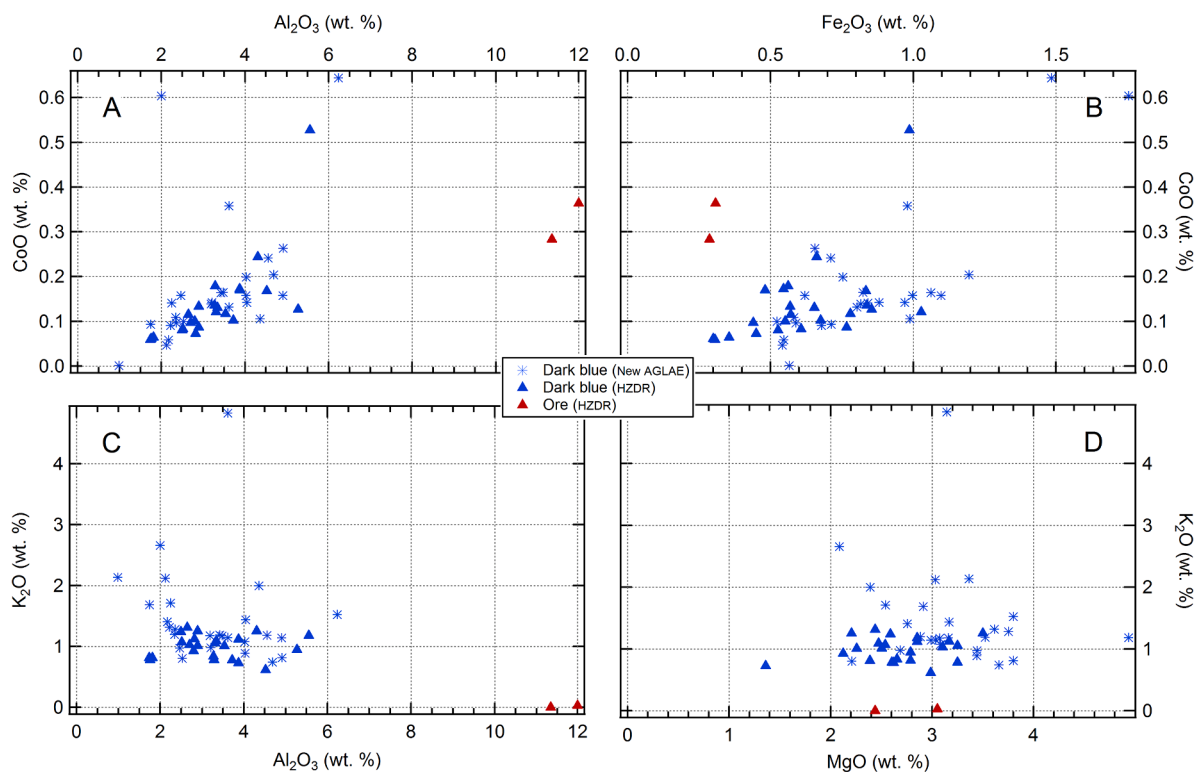


**Fig. 6.** Graphs showing (upper register) the correlation between CoO and Al<sub>2</sub>O<sub>3</sub> and Fe<sub>2</sub>O<sub>3</sub>, both of which are particularly clear for the blue Co- and Co-Cu coloured objects as well as the ore from Dakhla Oasis, and (lower register) the correlation between K<sub>2</sub>O and Al<sub>2</sub>O<sub>3</sub> and MgO, highlighting the differences between the blue Co- and Co-Cu coloured objects. Graphs. F. Munnik/HZDR. (For interpretation of the references to colour in this figure legend, the reader is referred to the web version of this article.)

2012) based on a series of pXRF analyses conducted in Egypt (cf. Kaparou et al., 2023). The regions for the ore type have been taken from (Abe et al., 2012) and the values have been recalculated from oxide to elemental concentrations. For this recalculation, MnO has been taken as the oxide and not MnO/3 (as stated in Figs. 4 and 6 in Abe et al., 2012) because MnO<sub>3</sub> is an unusual form of manganese oxide and the authors use MnO throughout the rest of their paper. ‘Type A’ cobalt is derived from the Co-ore mined in the region of the Dakhla and Kharga Oases in the Egyptian western desert (see Fig. 1). This Co-ore was used for colouring glass and faience in the 18th Dynasty and which had already been noted by A. Kaczmarczyk (Kaczmarczyk, 1986; Shortland et al., 2006). The range covered by ‘Type A’ cobalt, which is characterised by a high Zn content, also includes the two Co-ore samples from the region of Ain Asil (Dakhla Oasis), which had been collected in the same region as the ores used to colour the glass (see Shortland et al., 2006).

‘Type N’ Co as described by Abe and colleagues also exists, and this is generally characterised by a low Ni content with a moderate Zn content, resulting in a pure Co colourant (Abe et al., 2012). Simultaneously, this type is either low or high in Mn, and correspondingly high or low in Co. Based on the latter it can be divided into two subgroups with a possible origin in Iran (‘Type N1’ (moderate-MnO and high-CoO) and ‘Type N2’ (high-MnO and low CoO: Abe et al., 2012)), neither of which were identified during the microPIXE-PIGE analyses.

A third type of Co, ‘Type R’ Co-ore was used to colourise a large amount of the Egyptian glass and faience dating to the Ramesside Period. While the chemical fingerprint of this ore overlaps with that of ‘Type A’, with similar correlations between Co-ore and the transition metals in general, it is also somewhat lower in Zn and Al (Abe et al., 2012).

An outlier is object ÄM 40418, a multi-coloured glass strip that was presumably produced in order to manufacture intricate mosaic glass

objects and / or jewellery (see Fig. 2). Based on its bright red colour and the combination of colours, i.e. stylistic details, this item can already be assigned to a later time, probably the Roman Period. In Fig. 5, this object can be identified based on its low Zn and Ni, and its relatively high Mn and Co content. It is not clear whether this object can be assigned to any other source of Co-ore, although it does appear to be close to Type R cobalt (cf. Hodgkinson et al., 2019a).

In general, 18th Dynasty Co-coloured glass objects are also recognisable by their high Mg and Al contents, the latter, similarly to Fe, positively correlating with Co. Objects coloured with Co are also generally low in potassium (K), this being due to the source of natron or plant ash used in its manufacture, although this is still under debate (see Shortland, 2012, 135). These characteristics coincide with those of Co-Cu coloured glass objects and can be observed in Fig. 6, this being most likely due to the fact that significant amounts of Cu were added to Co-coloured glass in order to achieve a different shade of blue (thus maintaining the overall characteristics of Co-coloured glass), rather than Co being added to Cu-coloured glass, although some Cu may be present in Co-coloured glass as another transition metal (see Smirniou and Rehren, 2013).

#### 4. Conclusion

In this paper the authors presented and discussed a summary of the microPIXE-PIGE analyses performed on 47 archaeological glass samples from the Ancient Egyptian site of Amarna, which are now kept in the collection of the Egyptian Museum and Papyrus Collection, Berlin. The composition of the analysed glass objects corresponds to that of Late Bronze Age / New Kingdom Egyptian soda-lime-silica glass. Twenty-six of the analysed samples are blue in colour, and this is due to the use of a Co-colourant. Thirteen of the glass objects are of other colours, ranging

from an intended colourless, translucent, over yellow, orange, red, violet to turquoise and green. The microPIXE-PIGE analyses permitted the determination of the minor and trace elements that are responsible for the colouration of these objects. They demonstrate the wide range of different compounds that were used in the sophisticated glass production at the site of Amarna as early as the 18th Dynasty (between 1550 and 1070 BCE) of the New Kingdom in Ancient Egypt.

The use of RBS technology permits the researcher to identify the extent and nature of the weathering (or corrosion) crust, which is chemically different from the core glass as well as providing information regarding the homogeneity of both the core glass matrix and the surface. Being able to determine the composition and thickness of this crust for a range of glass objects of the same colour makes it possible to extrapolate this information to other objects of the same colour and gain more information on the general composition of the glass and the environmental conditions of the archaeological context in which it was deposited.

Simultaneously, the microPIXE-imaging of the glass delivers information on the range of colourants included in polychrome glass objects, and on how the individual elements of such a piece of glass have bonded during the manufacturing process. Thus, microPIXE-imaging may provide information on ancient glass workshops and the choice of colours in the manufacture of glass objects.

The known correlations between Co and Mn, Zn, and Ni, which are derived from the Co-ore mined in the western oases of Egypt, have been possible to reconstruct using both the IBC, HZDR and the New AGLAE facility datasets. In addition, a positive correlation between Co and both Al and Fe can be observed, regardless of the dataset. These correlations can also be reproduced by LA-ICP-MS (Hodgkinson and Frick, 2020a), while the transition metal correlations alone are already reproducible by pXRF (Hodgkinson et al., 2019a). Furthermore, it has been established that the transition metals are sufficient to determine the source of the Co-ore, as has been demonstrated in the case of later glass object ÄM 40418, which contained Co from a different source than that used to colour the blue glass objects from the Amarna Period.

Although the objects analysed at IBC, HZDR and New AGLAE belong to a museum collection and have lost their archaeological context since being collected in Egypt and being brought to Germany at the beginning of the 19th century, it is at least possible to confirm the site of Amarna as their provenance, since the chemical fingerprint of these objects matches that of better provenanced items from the same site. In addition, both LA-ICP-MS and PIXE/PIGE have verified the pXRF data collected at Amarna, the same transition metal patterns emerging through all techniques, indicating that the source of the Co-ore was indeed the oases Kharga and Dakhla in the Egyptian western desert. As already outlined elsewhere (Hodgkinson et al., 2019a), the verification of the pXRF data by means of the above methods indicates that the source of the Co ore can be identified in the field, which is of great importance since the archaeological material has to remain in Egypt.

#### CRediT authorship contribution statement

**Anna K. Hodgkinson:** Conceptualization, Formal analysis, Funding acquisition, Investigation, Methodology, Project administration, Supervision, Validation, Visualization, Writing – original draft, Writing – review & editing. **Quentin Lemasson:** Formal analysis, Resources, Software, Visualization. **Michael Mäder:** Formal analysis, Resources, Software, Validation. **Frans Munnik:** Data curation, Formal analysis, Investigation, Resources, Software, Validation, Visualization, Writing – original draft, Writing – review & editing, Conceptualization. **Laurent Pichon:** Data curation, Formal analysis, Resources, Software, Validation, Visualization. **Stefan Röhrs:** Conceptualization, Formal analysis. **Ina Reiche:** Conceptualization, Data curation, Formal analysis, Investigation, Methodology, Project administration, Supervision, Validation, Writing – original draft, Writing – review & editing.

#### Declaration of Competing Interest

The authors declare that they have no known competing financial interests or personal relationships that could have appeared to influence the work reported in this paper.

#### Data availability

The research data is available in [table S2](#) of the Supplementary Materials.

#### Acknowledgements

The authors would like to thank both Friederike Seyfried and Nina Loschwitz (Ägyptisches Museum und Papyrussammlung, Staatliche Museen zu Berlin, Stiftung Preußischer Kulturbesitz) for providing access to the glass objects from Amarna in the collection of the Egyptian Museum, Berlin, and the excellence cluster Topoi (Freie Universität Berlin) for funding the research project on the provenance of the Co-ore (A-6-Cofund-1 and PLUS-8). The research team would also like to thank the Smithsonian Institute for providing the Corning A reference standards and the Corning Museum of Glass for providing the Corning B and D standards. Andrew Shortland is thanked for the loan of the two Co-ore samples originally collected by A. Kaczmarczyk.

The beamtime allowance at the Ion Beam Centre (IBC) of the HZDR through access proposal 18001342-ST is acknowledged and the operators of the IBC are thanked for producing the ion beams.

The ion beam analysis experiments were performed twice at the New AGLAE facility (ANR - 10 - EQPX 22). We acknowledge financial support of the European infrastructure program IPERION CH under the Grant agreement 392 no. 654028. The other New AGLAE team members, especially Claire Pacheco and Brice Moignard, are thanked for the support of this project before and during beamtime. We also thank Caroline Vibert, Master student at the Rathgen research laboratory (RRL), for the preliminary study of the objects at RRL. Finally, we are grateful to the editorial board of the Journal of Archaeological Science: Reports and to the two anonymous reviewers for their helpful comments.

#### Appendix A. Supplementary material

Supplementary data to this article can be found online at <https://doi.org/10.1016/j.jasrep.2024.104412>.

#### References

- Abe, Y., Harimoto, R., Kikugawa, T., Yazawa, K., Nishisaka, A., Kawai, N., Yoshimura, S., Nakai, I., 2012. Transition in the use of Cobalt-Blue Colorant in the New Kingdom of Egypt. *J. Archaeol. Sci.* 39 (6), 1793–1808. <https://doi.org/10.1016/j.jas.2012.01.021>.
- Barradas, N.P., Jeynes, C., Webb, R.P., 1997. Simulated annealing analysis of Rutherford backscattering data. *Appl. Phys. Lett.* 71 (2), 291–293. <https://doi.org/10.1063/1.119524>.
- Borchardt, L., Ricke, H., 1980. *Die Wohnhäuser in Tell El-Amarna, Ausgrabungen der Deutschen Orient-Gesellschaft in Tell El-Amarna, Band V. Wissenschaftliche Veröffentlichungen Der Deutschen Orient-Gesellschaft 91*. Gebr. Mann, Berlin.
- Brill, R.H., 1999. *Chemical Analyses of Early Glasses, Vol. 2*. Corning Museum of Glass, Corning, N.Y.
- Calligaro, T., Coquinot, Y., Pichon, L., Moignard, B., 2011. Advances in elemental imaging of rocks using the AGLAE external microbeam. *Nucl. Instrum. Methods Phys. Res., Sect. B* 269 (20), 2364–2372.
- Campbell, J.L., Hopman, T.L., Maxwell, J.A., Nejedly, Z., 2000. The Guelph PIXE Software Package III: Alternative Proton Database. *Nucl. Instrum. Methods Phys. Res., Sect. B* 170 (1–2), 193–204. [https://doi.org/10.1016/S0168-583X\(00\)00156-7](https://doi.org/10.1016/S0168-583X(00)00156-7).
- Campbell, J.L., Boyd, N.I., Grassi, N., Bonnicks, P., Maxwell, J.A., 2010. The Guelph PIXE Software Package IV. *Nucl. Instrum. Methods Phys. Res., Sect. B* 268 (20), 3356–3363.
- Hodgkinson, A.K., Bertram, M., 2020. Working with fire: Making glass beads at Amarna using methods from metallurgical scenes. In: Rademakers, F.W., et al. (Eds.), *Contributions of Experimental Archaeology to Excavation and Material Studies*.

- Journal of Archaeological Science: Reports 33, 102488. <https://doi.org/10.1016/j.jasrep.2020.102488>.
- Hodgkinson, A.K., Röhrs, S., Müller, K., Reiche, I., 2019a. The use of Cobalt in 18th Dynasty Blue Glass from Amarna: the results from an on-site analysis using portable XRF technology. *STAR: Sci. Technol. Archaeol. Res.* 5 (2), 36–52. <https://doi.org/10.1080/20548923.2019.1649083>.
- Hodgkinson, A.K., Röhrs, S., Müller, K., Reiche, I., 2019b. Portable X-Ray Fluorescence Analysis of Late Bronze Age Glass from Amarna. Data publication. Edition Topoi. <https://doi.org/10.17171/2-15>.
- Hodgkinson, A.K., Frick, D.A., 2020a. Identification of Co-Coloured Egyptian Glass Objects by LA-ICP-MS: A Case Study from the 18th Dynasty Workshops at Amarna, Egypt. *Mediterr. Archaeol. Archaeom.* 20 (1), 45–57. <https://doi.org/10.5281/zenodo.3605660>.
- Hodgkinson, A.K., Frick, D.A., 2020b. 'Data Set of Major, Minor and Trace Elements in Co-Coloured Egyptian Glass Objects from the 18th Dynasty Workshops at Amarna. Egypt' <https://doi.org/10.5880/GFZ.3.3.2019.001>.
- Janssens, K. (Ed.), 2013. *Modern Methods for Analysing Archaeological and Historical Glass, Volume 1*. Wiley, Chichester, West Sussex, United Kingdom.
- Kaczmarczyk, A., 1986. The Source of Cobalt in Ancient Egyptian Pigments. In: Olin, J.S., Blackman, M.J. (Eds.), *Proceedings of the 24th International Archaeometry Symposium*. Smithsonian, Washington D.C., pp. 369–376.
- Kaparou, M., Tsampa, K., Zacharias, N., Karydas, A.G., 2023. Analytical exploration of the mycenaean glass world via Micro-PIXE: a contribution to our knowledge of LBA glass technology. *Archaeol. Anthropol. Sci.* 15 (12), 201. <https://doi.org/10.1007/s12520-023-01898-y>.
- Kemp, B.J., Garfi, S., 1993. *A Survey of the Ancient City of El-'Amarna*. Occasional Publication 9. Egypt Exploration Society, London.
- Lankton, J.W., Pulak, C., Gratzue, B., 2022. Glass Ingots from the Uluburun Shipwreck: Glass by the Batch in the Late Bronze Age. *J. Archaeol. Sci. Rep.* 42, 103354 <https://doi.org/10.1016/j.jasrep.2022.103354>.
- Mäder, M., Neelmeijer, C., 2004. Proton Beam Examination of Glass – an Analytical Contribution for Preventive Conservation. *Nucl. Instrum. Methods Phys. Res., Sect. B* 226 (1–2), 110–118.
- Matin, M., 2019. Tin-based opacifiers in archaeological glass and ceramic glazes: a review and new perspectives. *Archaeol. Anthropol. Sci.* 11 (4), 1155–1167.
- Neelmeijer, C., Wagner, W., Schramm, H.P., 1996. Depth Resolved Ion Beam Analysis of Objects of Art. *Nucl. Instrum. Methods Phys. Res., Sect. B* 118 (1), 338–345. [https://doi.org/10.1016/0168-583X\(95\)01193-5](https://doi.org/10.1016/0168-583X(95)01193-5).
- Nicholson, P.T., 2007. *Brilliant Things for Akhenaten: The Production of Glass, Vitreous Materials and Pottery at Amarna Site O45.1*. Excavation Memoir 80. The Egypt Exploration Society, London.
- Nicholson, P.T., Henderson, J., 2000. Glass. In: Nicholson, P.T., Shaw, I.M.E. (Eds.), *Ancient Egyptian Materials and Technology*. Cambridge University Press, Cambridge, pp. 195–224.
- Pichon, L., Moignard, B., Lemasson, Q., Pacheco, C., Walter, P., 2014. Development of a multi-detector and a systematic imaging system on the AGLAE external beam. *Nucl. Instrum. Methods Phys. Res., Sect. B* 318, 27–31.
- Pichon, L., Calligaro, T., Lemasson, Q., Moignard, B., Pacheco, C., 2015. Programs for Visualization, Handling and Quantification of PIXE Maps at the AGLAE Facility. *Nucl. Instrum. Methods Phys. Res., Sect. B* 363, 48–54.
- Rehren, Th., 2001. Aspects of the Production of Cobalt-Blue Glass in Egypt. *Archaeometry* 43 (4), 483–489. <https://doi.org/10.1111/1475-4754.00031>.
- Shortland, A.J., 2012. Lapis Lazuli from the Kiln: Glass and Glassmaking in the Late Bronze Age. Leuven University Press, Leuven.
- Shortland, A.J., Eremin, K., 2006. The analysis of second millennium glass from Egypt and Mesopotamia, Part 1: New WDS Analyses. *Archaeometry* 48 (4), 581–603. <https://doi.org/10.1111/j.1475-4754.2006.00274.x>.
- Shortland, A.J., Rogers, N., Eremin, K., 2007. Trace Element Discriminants between Egyptian and Mesopotamian Late Bronze Age Glasses. *J. Archaeol. Sci.* 34 (5), 781–789. <https://doi.org/10.1016/j.jas.2006.08.004>.
- Shortland, A.J., Tite, M.S., Ewart, I., 2006. Ancient exploitation and use of cobalt alums from the Western Oases of Egypt. *Archaeometry* 48 (1), 153–168.
- Smirniou, M., Rehren, Th., 2013. Shades of Blue - Cobalt-Copper Coloured Blue Glass from New Kingdom Egypt and the Mycenaean World: A Matter of Production or Colourant Source? *J. Archaeol. Sci.* 40 (12), 4731–4743. <https://doi.org/10.1016/j.jas.2013.06.029>.
- Swann, C.P., Fleming, S.J., 1987. Proton-Induced X-Ray Emission Spectrometry in Archaeology. *Scanning Microsc.* 2 (1), 197–207.
- Tite, M., Pradell, T., Shortland, A.J., 2008. Discovery, production and use of tin-based opacifiers in glasses, enamels and glazes from the late iron age onwards: a reassessment\*. *Archaeometry* 50 (1), 67–84.
- Vicenzi, E.P., Eggins, S., Logan, A., Wysoczanski, R., 2002. Microbeam characterization of corning archaeological reference glasses: new additions to the smithsonian microbeam standard collection. *J. Res. Natl. Inst. Standards Technol.* 107, 719–727.
- Wagner, B., Nowak, A., Bulska, E., Hametner, K., Günther, D., 2012. Critical assessment of the elemental composition of Corning archaeological reference glasses by LA-ICP-MS. *Anal. Bioanal. Chem.* 402 (4), 1667–1677.
- Wang, Y., Nastasi, M., 2009. *Handbook of Modern Ion Beam Materials Analysis*, 2nd ed. Materials Research Society, Warrendale, Pennsylvania.
- Ziegler, J.F., Ziegler, M.D., Biersack, J.P., 2010. SRIM – The Stopping and Range of Ions in Matter (2010). *Nucl. Instrum. Methods Phys. Res., Sect. B* 268 (11–12), 1818–1823. <https://doi.org/10.1016/j.nimb.2010.02.091>.